7th IFAC Conference on Manufacturing Modelling, Management, and Control
International Federation of Automatic Control
June 19-21, 2013. Saint Petersburg, Russia

Robot Joint Modeling and Parameter Identification Using the Clamping Method ⋆

Christian Lehmann * **Björn Olofsson** ** **Klas Nilsson** ***
Marcel Halbauer * **Mathias Haage** *** **Anders Robertsson** **
Olof Sörnmo ** **Ulrich Berger** *

* *Chair of Automation Technology, Brandenburg University of Technology, D–03046 Cottbus, Germany. E-mail: lehmann.christian@tu-cottbus.de.*
** *Department of Automatic Control, LTH, Lund University, SE–221 00 Lund, Sweden. E-mail: bjorn.olofsson@control.lth.se.*
*** *Department of Computer Science, LTH, Lund University, SE–221 00 Lund, Sweden. E-mail: klas.nilsson@cs.lth.se.*

Abstract: The usage of industrial robots for milling tasks is limited by their lack of absolute accuracy in presence of process forces. While there are techniques and products available for increasing the absolute accuracy of free-space motions, the mechanical weaknesses of the robot in combination with the milling forces limits the achievable performance. If the dynamic effects causing the deviations can be compensated for, there would be several benefits of using industrial robots for machining applications. To enable the compensation, the causes of the path deviations have to be adequately modeled, and there must be a method for determining the model parameters in a simple and inexpensive way. To that end, we propose a radically new method for identification of robot joint model parameters, based on clamping of the robot to a rigid environment. The rigidity of the environment then eliminates the need for expensive measurement equipment, and the internal sensors of the robot give sufficient feedback. An experimental validation shows the feasibility of the method.

1. INTRODUCTION

As a result of the increased demand on cost-efficiency and flexibility in the manufacturing industry, the interest in utilizing industrial robots as a complement to dedicated machine tools for high-end machining tasks, such as milling and deburring, has increased over the past decade. However, considering the strong process forces required for this kind of tasks, this has for a long time been hampered by the compliance of the robot joints, limited Cartesian position accuracy and comparably low structural bandwidth of the robot (Abele et al., 2008; Wang et al., 2009; Pan and Zhang, 2009).

Within the EU-funded project COMET (COMET, 2013), the aim is to develop milling solutions with industrial robots achieving an accuracy better than 50 µm. One step towards achieving this accuracy is to develop a model-based path planning algorithm for milling tasks. This poses two problems to be solved: 1.) The development of a model of the relevant robot characteristics and a subsequent method for identification of the model parameters for an arbitrary industrial robot. 2.) Utilization of the robot model in the offline path-planning stage for increasing the resulting machining accuracy. The focus of the current paper is on the former task. The second problem will be addressed in a future paper.

This paper is outlined as follows. A background to the investigated problem is given in Sec. 2, followed by a description of the adopted modeling approach in Sec. 3. Section 4 presents the parameter identification approach based on clamping of the robot to a rigid environment and the method is subsequently experimentally evaluated in Sec. 5. A discussion of the method and the experimental results are provided in Sec. 6. Finally, conclusions and aspects on future work are given in Sec. 7.

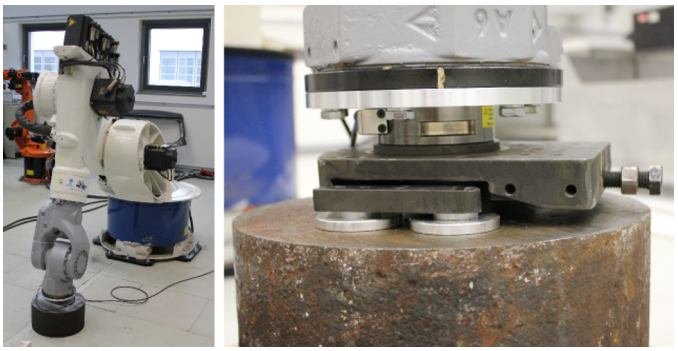

Fig. 1. Clamping of the end-effector of the robot to the environment, with a F/T-sensor mounted between end-effector and fixture.

2. BACKGROUND

The usage of industrial robots for milling tasks is limited by their lack of absolute accuracy and therefore the ability to perform manufacturing based on CAD-specifications. Further, the mechanical weaknesses of the structure of the robot limits the achievable performance. If these drawbacks can be compensated for, several benefits of industrial robots can be identified: Large workspace, comparably low investment costs, high flexibility, reconfigurability, and versatility.

⋆ The research work reported here was supported by the European Commission under the Seventh Framework Programme (FP7/2007-2013) within the project COMET under grant agreement #258769.

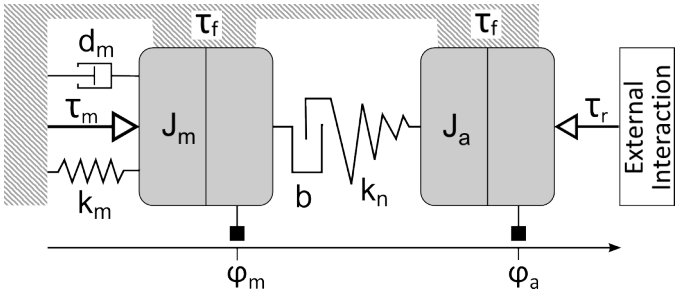

Fig. 2. Joint model including backlash, friction on motor and arm side, and nonlinear stiffness. The joint is depicted as a prismatic joint for simplicity.

Besides the need for high absolute accuracy and consideration of process forces, the characteristics of machining applications differ from conventional robot tasks in free space, like pick-and-place applications: The velocities of the robot joints are comparably low; therefore the dynamic influences of mass and inertia of the robot arm have less effect on the positioning and path accuracy. Additionally, a stable end-effector velocity is required since any change of cutting feed leads to varying cutting conditions and therefore non-uniform machining quality. Further, no online correction of single program points is possible, only an initial offset can be applied during calibration of the tool and workpiece reference points. Therefore any calibration or compensation approach, based on off-line corrections, has to be applied to the tool path as a whole.

3. MODELING APPROACH

The model developed in this paper is opted for describing the characteristics of the robot in a milling scenario. Hence, the pure kinematic representation of the robot structure is insufficient, since it does not consider nonlinear dynamics and flexibilities in the joints. To a large extent, the position errors of the robot occurring in milling tasks are to be attributed to effects in the robot joints (Zhang et al., 2005). As stated earlier, the robot velocity during milling is moderate under normal operation, hence the inertial effects caused by the mass of the links can be neglected.

The most prominent effects in the robot joints, influencing the resulting milling performance, are identified from extensive milling experiments, performed with industrial robots, as the following:

- Backlash of the gearbox;
- Static and dynamic friction within the joint;
- Nonlinear stiffness of the joint.

Consequently, the model proposed in this paper is a joint-based robot model containing the elements above. The model components for each of the joints are schematically described in Fig. 2. The corresponding notations for variables and parameters are collected in Table 1. Since the link effects are omitted—or to some extent included in the joint dynamics—in the proposed robot model for milling scenarios, each joint is modeled independently of the others. However, cross-coupling between the joints can be introduced as external disturbances in each joint model. The main model components for each joint are discussed next.

Table 1. Variables and parameters in joint model.

τ_m	—	Torque from controller to motor
τ_r	—	Reaction torque from fixture
φ_m	—	Joint angle, motor side
φ_a	—	Joint angle, arm side
b	—	Backlash
k_n	—	Nonlinear spring constant
τ_f	—	Friction torque
J_m	—	Actuator/motor inertia
J_a	—	Arm side inertia
k_m	—	Stiffness accomplished by controller
d_m	—	Damping accomplished by controller

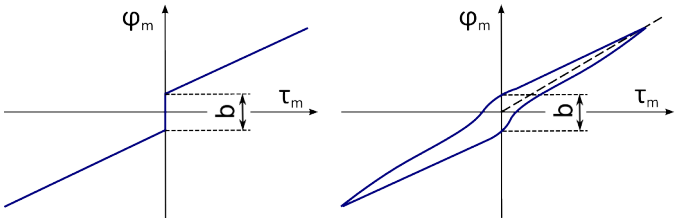

Fig. 3. Left picture: In theory no torque is required to move through the backlash of the robot joint. Right picture: A more realistic depiction of the behavior of a gear, including the backlash traversal (Neugart, 2002).

3.1 Backlash

For the most simple gears, backlash is the shortest distance or clearance between non-driving teeth in mating gears (Hovland et al., 2002). When the motion of the gear is reversed, part of the motion is lost because of the backlash. When traversing the backlash in the robot joint, the motion can be depicted as in the left plot in Fig. 3. However, because of non-ideal backlash contact, hysteresis, and internal friction in the gearbox, the ideal motion through the backlash is not obtained in practice. Rather, a behavior similar to the right plot in Fig. 3 is obtained. Each joint of the robot is in the model characterized by its backlash angle, corresponding to the lost motion occurring when the gear motion is reversed.

3.2 Static and Dynamic Friction

Robot joints also exhibit static and dynamic friction dynamics. A friction model for industrial robot joints, including viscous as well as Stribeck effects, is presented in (Bittencourt et al., 2010). The model considers the friction dynamics in steady state as function of the joint angle velocity. This model strategy is adopted in this paper. In the model, the friction torque τ_f for each joint is described as function of the motor angular velocity $\dot{\varphi}_m$, see Fig. 4, according to the following relation

$$\tau_f(\dot{\varphi}_m) = \left(F_C + F_S e^{-\left|\frac{\varphi_m}{\varphi_S}\right|^{\alpha}}\right)\mathrm{sign}(\dot{\varphi}_m) + F_V\dot{\varphi}_m, \qquad (1)$$

where $F_C, F_S, \dot{\varphi}_S, \alpha$, and F_V are model parameters to be determined from experimental data. For further details of the friction measurement method, see (Bittencourt et al., 2010).

3.3 Joint Stiffness

The stiffness of the robot joint characterizes the relationship between applied torque and the corresponding angular rotation. In its most idealized form, this relationship is linear but in practice this relation is often characterized by nonlinear components. An equivalent representation of the torque–position

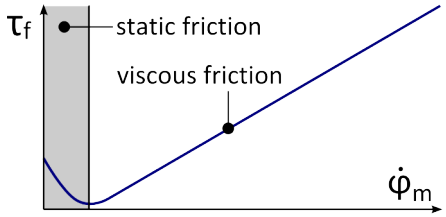

Fig. 4. Friction behavior as described in (Bittencourt et al., 2010).

relationship in the joint, is the so called joint compliance which is the inverse of the joint stiffness. This quantity is commonly used to describe this part of the robot joint behavior. However, from a joint modeling point-of-view and subsequent simulation perspective, the joint stiffness is to be preferred in this model. In practice, the stiffness relationship for each joint is characterized by a torque-position map, experimentally determined from measurement data, which is further elaborated in Sec. 4.4.

4. PARAMETER IDENTIFICATION

In this section, a measurement procedure for establishing the main parameters of the robot joint model described in the previous section is presented. Measurement of the backlash and the joint stiffness are based on rigidly clamping the robot to the environment (Nilsson, 2012), whereas the friction is measured by motion in free space.

4.1 Clamping Method

Measurement of robot stiffness and backlash values are traditionally performed by applying a load on the robot tool center point (TCP) and then measure the resulting end-effector force and torque with a Force/Torque-sensor (F/T-sensor), attached to the robot wrist. Simultaneously, the corresponding deflection of the robot end-effector is measured using expensive high-resolution measurement equipment, such as optical tracking systems or arm-side encoders (Wang et al., 2009; Pan and Zhang, 2009; Ruderman et al., 2009). On the contrary, by rigidly attaching the TCP of the robot to the environment, there is no longer a need to measure its position with an external measurement equipment, which reduces the costs for the setup as well as the error sources. A method for kinematic calibration based on clamping of the robot was proposed in (Bennett et al., 1992). In this paper we apply that principle to the measurement of joint backlash and stiffness, which we in turn think will facilitate the practical use of the kinematic clamping method—which in that paper was only simulated with ideal joint properties.

Two different approaches for realization of the clamping procedure were developed: The first was using a tool-change system to lock the robot to the environment that it was docked onto using a force-control strategy for position control of the robot to automatically insert the TCP in that tool change system from an arbitrary initial position. The force-control strategy was based on impedance control (Siciliano and Villani, 1999). The second approach was realized in a simpler way in order to avoid the need for low-level robot controller access: A metal plate, which was mounted on the end-effector, was manually screwed to the rigid environment. The robot was then moved manually, using incremental moves, to adjust the initial tension on the F/T-sensor. Both methods were used during the experimental validation, see Sec. 5.

4.2 Measurement of Backlash

In order to measure the backlash value for each joint, the robot was rigidly attached to the environment as described above, so that the gear in the joint should move like in free-space motion within the backlash, but encounter resistance to the movement as soon as the backlash is left. While the robot was clamped, each joint was moved back and forth, one joint at a time. Motor position and current, or torque values if these are available for measurement, were logged.

The magnitude of the possible angular displacement of each joint with this method is limited by the maximum possible force that can be applied to the F/T-sensor mounted at the end-effector. Therefore, robot configurations which result in a small leverage between the moved joint and the end-effector are to be preferred in order to obtain measurement data for a larger interval of the joint positions.

An angular position to torque behavior similar to the one depicted in Fig. 3 was expected; but as a F/T-sensor was mounted on the end-effector, the joint movements were limited by the maximum force which could be applied to that sensor. Therefore, only the center part of the diagram shown in Fig. 3 is included in the measured data.

4.3 Measurement of Joint Friction

To determine the parameters of the friction model, motions in free space were executed with each of the robot joints. After a warm-up procedure, each joint was moved in a position interval

$$\left[-\varphi_m^{(f)}, \varphi_m^{(f)}\right],$$

with increasing motor velocities. For each velocity, the respective required torque was logged; a set of measurements over the whole velocity range of a joint then describes its steady state friction behavior. For further details on the friction measurement method, the reader is referred to (Bittencourt et al., 2010).

4.4 Measurement of Joint Stiffness

In order to determine the torque-position map for each joint, the robot was clamped to the environment with the F/T-sensor attached, as described in Sec. 4.1. The following procedure was executed for each joint: First the motion limits for the joint in the clamped position were determined. Each deviation of the joint position from the initial position in that configuration results in a force applied to the F/T-sensor attached to the end-effector. The limits of applicable force on the sensor therefore defined the limits of the joint movements; in order to get a maximum number of data points for all joints, re-clamping of the robot in different configurations and positions is to be preferred.

For the measurement itself, the joint was moved back and forth within the given limits, while the force at the end-effector and the motor position φ_m were recorded. Using the gear ratios of each joint, the corresponding joint position φ_a was calculated based on the measured motor position. Based on the measured force and the leverage between the mounting point of the F/T-sensor and the joint, the torque τ_a on the arm side of the respective joint can be calculated. Calculation of the leverage can be done using CAD data of the robot. If it is possible to only utilize torque data from the joint motor side instead of data

from the F/T-sensor, is subject to ongoing research. By applying a polynomial fit, a third-order polynomial

$$p(\Delta\varphi) = p_3(\Delta\varphi)^3 + p_2(\Delta\varphi)^2 + p_1(\Delta\varphi),$$

is determined for each joint, describing the stiffness $p(\Delta\varphi)$ as function of the angle difference $\Delta\varphi = \varphi_a - \varphi_m$.

5. EXPERIMENTAL SETUP AND RESULTS

In this section the experimental setups that were used for development and validation of the identification method, as proposed in Sec. 4, are described and a complete set of experimental results for one of the setups is presented.

Experimental validation was done on two different robots:

(1) KUKA KR125 (125 kg payload) with KRC1 controller; equipped with ATI FTD Delta-SI-660-60 F/T-sensor;
(2) ABB IRB2400 (16 kg payload) with S4CPlus controller and ExtCtrl research interface (Blomdell et al., 2010); equipped with JR3 100M40A F/T-sensor.

Besides the data from the respective F/T-sensor, access to robot controller data, such as logging of joint positions and motor currents, is required for the parameter identification. For the first setup, the ExtCtrl controller interface was used to access these values. However, ExtCtrl is a research interface and not a standard ABB interface; for an introduction to the ExtCtrl interface, the reader is referred to (Blomdell et al., 2010). In the second setup, the internal "oscilloscope" function of KUKA was used to create the respective log files.

5.1 Clamping Procedure

The automated clamping method, as described in Sec. 4.1, was implemented on the ABB setup. The time required for clamping the robot in a given configuration is approximately 30–60 seconds, depending on the initial robot pose. With this approach, no user interaction besides defining the approaching direction towards the target position was required. On the KUKA setup the manual clamping procedure, as depicted in Fig. 1, was utilized. Because of the involved manual steps, the time required for clamping in an arbitrary position was noticeably longer, 10–15 minutes. In the demonstration setup, the initial tension on the F/T-sensor at the end-effector could be reduced to less than 1 N per spatial direction.

5.2 Parameter Identification

Parameter identification was done on both setups described above. In the following, the experimental results from the second setup with the KUKA KR125 robot are described, as they describe the approach required for an arbitrary robot, not relying on a non-standard controller interface.

Friction Measurements The friction measurements were performed in steps of 10 % of the stated maximum velocity—*i.e.*, 1.5–4.4 rad/sec, depending on joint. For the lower joint velocities (1–5 %) the step size was reduced to 1 % in order to capture the inherent Stribeck effect. The following observations were made: 1.) The Stribeck effects, as depicted in Fig. 4, were almost not recognizable for most of the joints on the KUKA robot. However, on the mentioned ABB robot they were indeed identifiable. 2.) The measured velocities have to be logged for verification of the measurements, as for certain joints the stated maximum velocities cannot be achieved in practice, thus resulting in false data points when relying only on the programmed velocities.

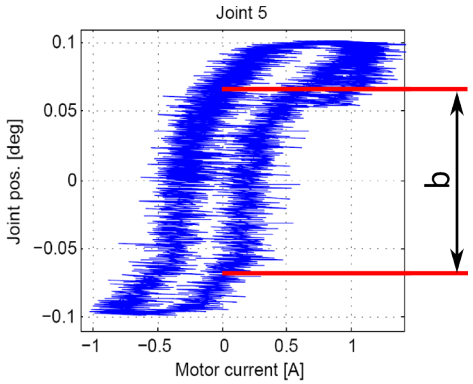

Fig. 5. Identification of the backlash value b based on the experimentally measured data.

Backlash Measurements The F/T-sensor mounted on the end-effector limited the movement for each joint to a corresponding joint angle of circa $\pm\, 0.1°$. The limitation of the angular movement is depending on the leverage of the respective joint and thus on the pose the robot is clamped in. Therefore, multiple clamping positions are to be preferred in order to get accurate results for all joints. As can be observed in the logged data, the recorded motor current signals contained a significant noise component; in order to reduce error influences and to improve the quality of the data, joint velocity and acceleration were reduced to 5 % of the respective maximum value. In addition, averaging over several motion cycles reduces the noise influence on the backlash identification. The results of the measurement for all six joints of the robot are displayed in Fig. 6. With the logged data, the backlash value for the joint is determined as depicted in Fig. 5. The result of this processing of the data for the measurements on the current robot is collected in Table 2.

Stiffness Measurements The required motion of the joints to capture the stiffness data is the same as for the backlash measurements, therefore data for both parameters can be captured at once. Clamping the robot in multiple configurations increases in importance here, as each joint movement is mapped to one force coordinate of the F/T-sensor. An exception here is joint 6, where the applied torque could directly be recorded as torque about the z-axis of the sensor. Ideally, the direction of the measured force is tangential to the rotational direction of the joint. Realization of this for all six joints requires clamping in different positions. In the experimental validation so far, measurements in three different positions were performed. However, the number of possible positions and configurations is currently limited by the realization of the fixture mechanism, see Fig. 1. The results from the experiments are displayed in Fig. 7. For each of the joints, a third-order polynomial fit using the least-squares method was computed. The fitted polynomial is also displayed in Fig. 7. The coefficients of the polynomial approximations are provided in Table 2.

6. DISCUSSION

In this section the experimental results presented in Sec. 5 are analyzed and discussed. Possible error sources and possibilities for improvement of the identification procedure are discussed.

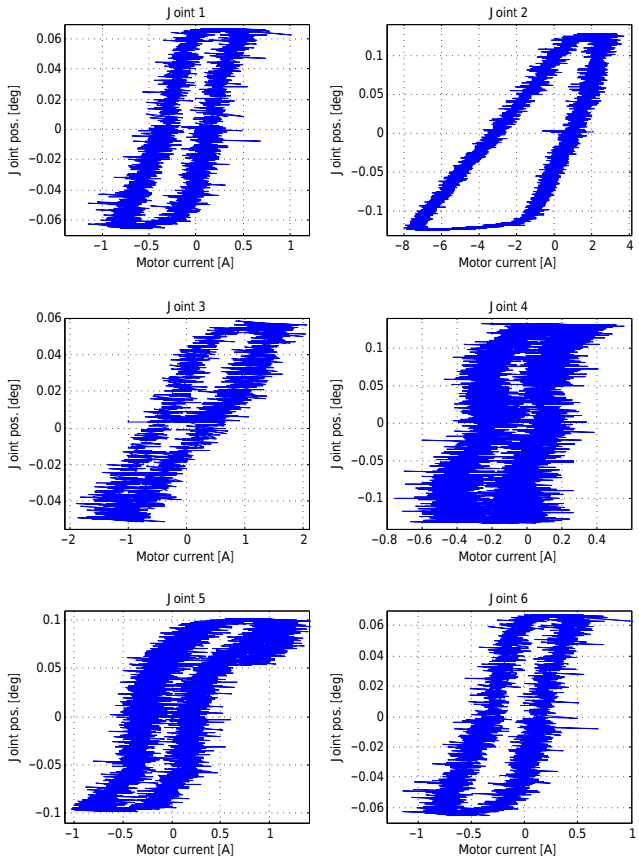

Fig. 6. Result of backlash measurements for KUKA KR125.

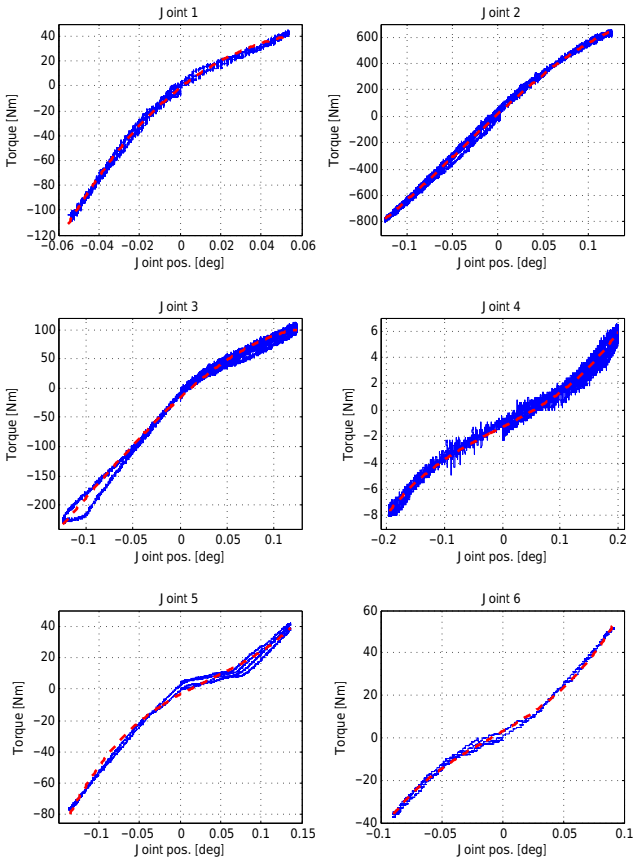

Fig. 7. Result of stiffness measurements on KUKA KR125 robot. The polynomial approximations are indicated in dashed red.

Table 2. Results of backlash identification and polynomial approximation of the stiffness behavior of the joints of the KUKA KR125 robot.

Joint No.	Backlash [deg]	Stiffness function [10^3 Nm]
1	0.10	$28.7\varphi_a^3 - 10.9\varphi_a^2 + 1.30\varphi_a$
2	0.15	$-42.5\varphi_a^3 - 5.30\varphi_a^2 + 6.35\varphi_a$
3	0.10	$-8.72\varphi_a^3 - 3.14\varphi_a^2 + 1.47\varphi_a$
4	0.16	$0.304\varphi_a^3 + 0.00706\varphi_a^2 + 0.0225\varphi_a$
5	0.14	$8.04\varphi_a^3 - 0.921\varphi_a^2 + 0.285\varphi_a$
6	0.10	$19.9\varphi_a^3 + 0.598\varphi_a^2 + 0.331\varphi_a$

Backlash Identification The accuracy of the determined backlash values is limited to a resolution of approximately 0.01° because of the noise in the motor current signal and the quantization of the joint position encoders and the joint position controllers. By decreasing the gain of the joint position controllers, the quantization effects can be reduced. In addition, some dependency on the chosen clamping position is observed in the experiments. The variance of the observed values for different measurements in one of the configurations is low. However, there can be a noticeable variance between the measured joint backlash values in different configurations, if the motion limits for that particular joint are small in one of the poses. Repetition of the measurements in several positions can be used to identify these unfavorable poses and to exclude the results for the affected joints when processing the results of the identification procedure. In Fig. 8 the ranges of detected backlash values for measurements in two different poses are depicted. For comparison, the estimated backlash values are also depicted. It can be observed, that one of the poses gave much lower results for joint 2 and 3 than in the other position. For that salient position only small movements of joints 2 and 3, which were not significantly larger than the size of the detected backlash values, were possible. A F/T-sensor with a larger measurement range can be an improvement here and is to be preferred anyhow in order to increase the quality of the captured data.

Stiffness Identification The results from the stiffness measurements, as shown in Fig. 7, in general correlate with the expected stiffness behavior—the joint torque progressively increases with the deviation from the initial joint position. In addition, the nonlinear behavior of the robot joint is clearly visible. However, for some joints, *e.g.*, joint 2, the observed behavior is still very close to linear; in these cases it seems that the joint is not excited far enough to get into the area where the increasing slope of the torque curve is more pronounced. Again, the usage of a larger scaled F/T-sensor is likely to improve the quality of the acquired data.

For the examined robot, a comparably low stiffness was measured for joint 4. A possible reason for this phenomenon is that in none of the used clamping positions, joint 4 and 6 were completely orthogonal, so movement of joint 4 could as well excite movement in joint 6 and thus reduce the measured forces at the end-effector. The limitations of the current setup in terms of possible clamping positions are a drawback here. The stiffness function determined for joint 4 therefore has to be taken with reservations until modification of the experimental setup allow appropriate clamping positions and thus further investigations.

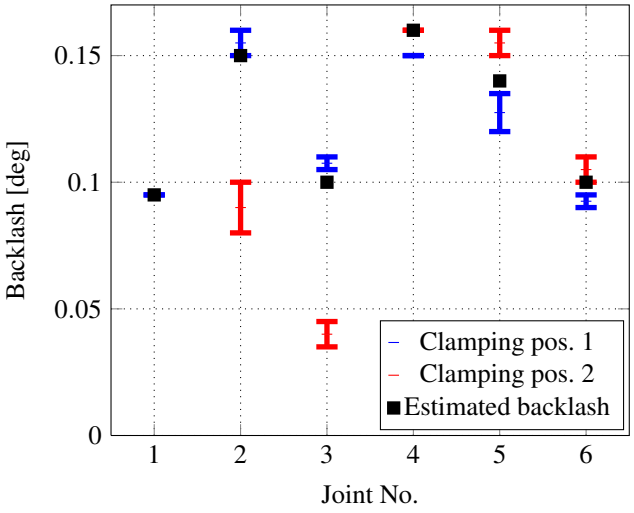

Fig. 8. Comparison of identified backlash values from two different clamping positions. The uncertainty interval caused by the inherent noise level in the measurements is also indicated for each data point.

As the access to controller parameters, such as motor current and joint position, is a prerequisite for utilization of the proposed parameter identification method, it can not be applied to robots where this access is not given. On the other hand, the parameter identification using the clamping method—if applicable—has a drastically decreased need for extensive measurement equipment compared to other identification methods, as described in Sec. 4.1.

7. CONCLUSIONS AND FUTURE WORK

In this paper, a new method for identification of robot joint model parameters was presented. The core of the method is the clamping of the robot end-effector to a rigid environment. Based on data acquired from the robot controller, specifically the joint positions, velocities, and motor currents, as well as forces and torques measured simultaneously at the end-effector, the parameters for a robot joint model describing joint friction, joint backlash, and joint stiffness were determined. The method proposed in (Bennett et al., 1992) for kinematic calibration on the clamped robot was taken as inspiration for doing a corresponding inversion of the problem for the identification of the joint parameters for backlash and stiffness. Experimental identification of these parameters was possible, although prospects for improvements have been identified in the experimental setup. The maximum measurement range of the F/T-sensor was a limiting factor in the experimental identification of the model parameters. Repeated measurements in different configurations using a sensor with a larger measurement range are planned as future work in order to get more descriptive results, both for the backlash and stiffness measurements. An interesting possibility here is to do the clamping of the robot without the sensor attached and do the measurements only with internal controller data, thus eliminating the need for any additional measurement device. In the current experimental setup, the possibilities to clamp the robot in arbitrary positions are restricted. As clamping of the robot in multiple configurations is desirable to get a profound basis for the calculation of the model parameters, further work on the clamping mechanism itself, also striving for less manual intervention, will be done. By replacing the rigid fixture with an adjustable and lockable device, *e.g.*, a hexapod with lockable joints, arbitrary clamping positions would be possible, while the need to adjust the robot in the clamping position would be omitted. Considering this perspective, the development of a fully automated data acquisition and parameter identification procedure is possible.

Based on the results presented in this paper, it is foreseen that robots in the future by themselves, without additional external sensing, will be able to determine their own properties, which paves the way for a breakthrough in machining with robots.

REFERENCES

Abele, E., Rothenbücher, S., and Weigold, M. (2008). Cartesian compliance model for industrial robots using virtual joints. *Prod. Eng. Res. Devel.*, 2, 339–343.

Bennett, D., Hollerbach, J., and Henri, P. (1992). Kinematic calibration by direct estimation of the Jacobian matrix. In *Proc. IEEE Int. Conf. on Robotics and Automation (ICRA)*, 351–357. Nice, France.

Bittencourt, A.C., Wernholt, E., Sander-Tavallaey, S., and Brogårdh, T. (2010). An extended friction model to capture load and temperature effects in robot joints. In *Proc. IEEE/RSJ Int. Conf. on Intelligent Robots and Systems (IROS)*, 6161–6167. Taipei, Taiwan.

Blomdell, A., Dressler, I., Nilsson, K., and Robertsson, A. (2010). Flexible application development and high-performance motion control based on external sensing and reconfiguration of ABB industrial robot controllers. In *Proc. of the Workshop on "Innovative Robot Control Architectures for Demanding (Research) Applications—How to Modify and Enhance Commercial Controllers", IEEE Int. Conf. on Robotics and Automation (ICRA)*, 62–66. Anchorage, AK.

COMET (2013). EU/FP7-project: *Plug-and-produce COmponents and METhods for adaptive control of industrial robots enabling cost effective, high precision manufacturing in factories of the future*, Available: http://www.cometproject.eu, Mar. 14, 2013.

Hovland, G., Hanssen, S., Moberg, S., Brogårdh, T., Gunnarson, S., and Isaksson, M. (2002). Nonlinear identification of backlash in robot transmissions. ISR 2002 Int. Symp. on Robotics, Stockholm, Sweden.

Neugart (2002). Backlash. `http://www.neugartusa.com/Service/faq/Gear%20Backlash.pdf`.

Nilsson, K. (2012). Patent Application SE-1251196-0: Method and system for determination of at least one property of a manipulator.

Pan, Z. and Zhang, H. (2009). Improving robotic machining accuracy by real-time compensation. In *Proc. ICROS-SICE Int. Joint Conf. 2009*, 4289–4294. Fukuoka, Japan.

Ruderman, M., Hoffmann, F., and Bertram, T. (2009). Modeling and identification of elastic robot joints with hysteresis and backlash. *IEEE Trans. Ind. Electron.*, 56(10), 3840–3847.

Siciliano, B. and Villani, L. (1999). *Robot Force Control*. Kluwer Academic Publishers.

Wang, J., Zhang, H., and Fuhlbrigge, T. (2009). Improving machining accuracy with robot deformation compensation. In *Proc. IEEE/RSJ Int. Conf. on Intelligent Robots and Systems (IROS)*, 3826–3831. St. Louis, MO.

Zhang, H., Wang, J., Zhang, G., Gan, Z., Pan, Z., Cui, H., and Zhu, Z. (2005). Machining with flexible manipulator: Toward improving robotic machining performance. In *Proc. IEEE/ASME Int. Conf. Adv. Intelligent Mechatronics (AIM)*, 1127–1132. Monterey, CA.